Molecular Therapy
Nucleic Acids
Original Article

Establishment of a pancreatic cancer animal model using the pancreas-targeted hydrodynamic gene delivery method

Osamu Shibata,[1,3] Kenya Kamimura,[1,2,3] Yuto Tanaka,[1] Kohei Ogawa,[1] Takashi Owaki,[1] Chiyumi Oda,[1] Shinichi Morita,[1] Atsushi Kimura,[1] Hiroyuki Abe,[1] Satoshi Ikarashi,[1] Kazunao Hayashi,[1] Takeshi Yokoo,[1] and Shuji Terai[1]

[1]Division of Gastroenterology and Hepatology, Graduate School of Medical and Dental Sciences, Niigata University, Niigata, 1–757 Asahimachi–dori Chuo–ku, Niigata 951-8510, Japan; [2]Department of General Medicine, Niigata University School of Medicine, Niigata, 1–757 Asahimachi–dori Chuo–ku, Niigata 951-8510, Japan

This research developed an easy-to-use, reproducible pancreatic cancer animal model utilizing pancreas-targeted hydrodynamic gene delivery to deliver human pancreatic cancer-related genes to the pancreas of wild-type rats. *KRAS*^{G12D}-induced pancreatic intraepithelial neoplasia lesions showed malignant transformation in the main pancreatic duct at 4 weeks and developed acinar-to-ductal metaplasia, which led to pancreatic ductal adenocarcinoma within 5 weeks, and the gene combination of *KRAS*^{G12D} and *YAP* enhanced these effects. The repeat hydrodynamic gene delivery of *KRAS*^{G12D} + *YAP* combination at 4 weeks showed acinar-to-ductal metaplasia in all rats and pancreatic ductal adenocarcinoma in 80% of rats 1 week later. Metastatic tumors in the liver, lymph nodes, and subcutaneous lesions and nervous invasion were confirmed. *KRAS*^{G12D} and *YAP* combined transfer contributes to the E- to N-cadherin switch in pancreatic ductal adenocarcinoma cells and to tumor metastases. This pancreatic cancer model will speed up pancreatic cancer research for novel treatments and biomarkers for early diagnosis.

INTRODUCTION

Pancreatic ductal adenocarcinoma (PDAC) is a leading cause of cancer-related deaths worldwide,[1,2] and the development of effective therapies is an unmet clinical need. The lack of an appropriate pancreatic cancer model is the major drawback. The model must mimic human pancreatic cancer in molecular pathogenesis, histological features, and multi-step malignant transformation for tumor marker and therapy development. Currently available models include chemical carcinogen-induced animal models,[3–8] cancer cell line-based xenografts, patient-derived xenografts, and organoid models.[9] In addition, injection of adenovirus-expressing Cre recombinase into the pancreatic duct of *Hras* and *Kras* transgenic rats showed pancreatic neoplasia, which is considered to be a pancreatic cancer model.[10] However, these models fail to achieve the reproducibility, cost benefit, efficacy, and similarity with human PDAC necessary for the development of novel therapies and biomarkers. Therefore, novel pancreatic cancer animal models with simple, easy, and reproducible methods are essential.

With this aim, we applied the hydrodynamic gene delivery (HGD) method, which has been used successfully to develop mice liver cancer *in vivo* by delivering oncogenes, including *Yap*, *Ras*, and *Myc,* to the liver[11-13]. To utilize this method, we established pancreas-targeted HGD to wild-type rats. The major advantages of this procedure include safe and effective gene delivery in a pancreas-specific manner, and optimization of injection parameters achieved effective transgene expression *in vivo* with no leakage of the transgene to other organs.[14] For the transgenes, the *KRAS*^{G12D} variant is related to pancreatic intraepithelial neoplasia (PanIN), and this dosage activated PDAC occurrence in almost all pancreatic cancers.[10,15,16] Sequentially activated genes, including *CDKN2A*, *TP53*, *SMAD4*, and *YAP* genes, increase the malignant potential of the tumors and contribute to the development of later-stage pancreatic intraepithelial neoplasia (PanIN) and acinar-to-ductal metaplasia (ADM).[17–19] ADM is the initial stage of PDAC[15,20–22] and *YAP* showed high expression in PDAC contributing to malignant transformation and metastasis through epithelial-mesenchymal transition (EMT).[23–27] Interestingly, it has been reported that *YAP* is a critical oncogenic effector of *KRAS*^{G12D} for the development of PDAC and can be a promising therapeutic target for PDAC.[17,28] Therefore, in this study, we utilized the pancreas-targeted HGD to examine the development of *in vivo* pancreatic cancer models by delivering oncogenes, including *KRAS*^{G12D} and *YAP*.

RESULTS

Effect of the *in vivo* oncogene HGD on the oncogenic signaling pathway

To examine whether *in vivo* oncogene HGD could activate the following carcinogenic signaling pathway, the time-dependent gene expression of the KRAS-related signaling pathway was examined after

Received 8 January 2022; accepted 27 March 2022;
https://doi.org/10.1016/j.omtn.2022.03.019.

[3]These authors contributed equally

Correspondence: Kenya Kamimura, Division of Gastroenterology and Hepatology, Graduate School of Medical and Dental Sciences, Niigata University, Niigata, 1–757 Asahimachi–dori Chuo–ku, Niigata 951-8510, Japan.
E-mail: kenya-k@med.niigata-u.ac.jp

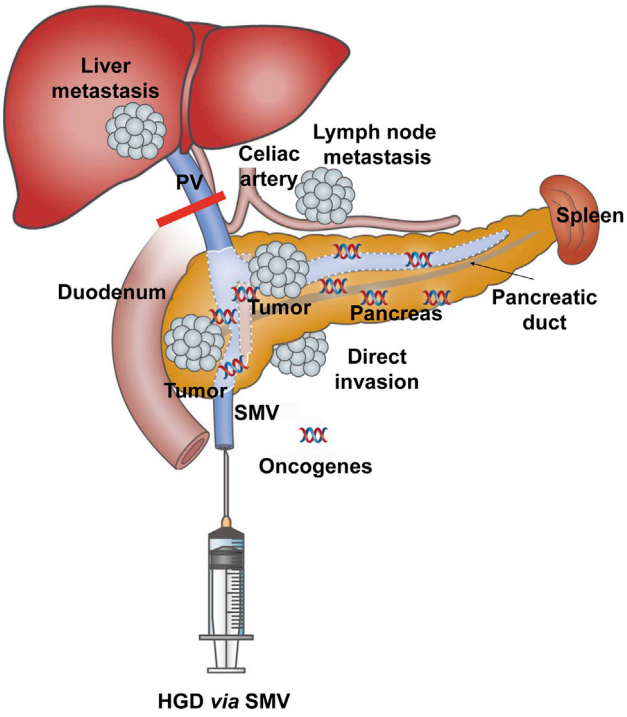

Figure 1. Schematic presentation of pancreas-targeted hydrodynamic gene delivery induced pancreatic cancer model

Schema of pancreas-targeted HGD of oncogenes from the SMV with a temporary vascular blockade at the PV. HGD, hydrodynamic gene delivery; HV, hepatic vein; PV, portal vein; SV, splenic vein; IVC, inferior vena cava; SMV, superior mesenteric vein.

pancreas-targeted HGD. The expressions of $KRAS^{G12D}$, Akt, Erk, Yap, Tgf-β1, and CTGF and the phosphorylation of Akt and Erk were assessed (Figure 2). Western blotting showed effective expression of $KRAS^{G12D}$, an increase of Akt, and phosphorylation of Akt 1 day after HGD, which was sustained for 5 days and decreased or was inactivated within 4 weeks. Erk showed a longer increase and phosphorylation duration, which was sustained for 4 weeks. Increased Yap, Tgf-β1, and Ctgf expressions were confirmed following the HGD of $KRAS^{G12D}$. HGD of the *YAP* gene showed increased Yap, Tgf-β1, and Ctgf expressions more clearly than KRAS HGD, while no increase of Kras, Akt, and Erk expression was seen (Figure 2A). Protein expression analyses *in vitro* using BxPC-3 and Panc-10.05, derived from pancreatic adenocarcinoma and hTERT-HPNE, with hTERT-immortalized pancreatic duct-derived epithelial cell used as a control, showed activation of Akt or Erk followed by the expressions of Yap, Tgf-β1, and Ctgf (Figure 2B). These results indicate that *in vivo* gene transfer of oncogenes to the pancreas achieved activation of the oncogene-related signaling pathway, which is activated in pancreatic cancer.

The effect of pancreas-targeted HGD of oncogene on pancreatic tumor development

To examine the effect of pancreas-targeted HGD of oncogenes on pancreatic tumor development, pancreatic carcinogenesis-related oncogenes of $KRAS^{WT}$, $KRAS^{G12D}$,[15,16,28,29] *MYC*,[30] and *YAP*[17,31] were hydrodynamically transferred to the wild-type rat pancreas, following a previously reported method,[14] which is briefly described in the materials and methods section (Figure 1). The plasmids were injected either individually or in combination (Figure 3A). $KRAS^{G12D}$ single gene delivery showed the development of some but not all macroscopic nodular lesions (Figure 3B), and all pancreatic tissues were harvested regardless of the mass development 4 weeks after HGD during the active period of transferred gene expression, as shown in Figure 2. Main pancreatic ducts were stained with hematoxylin and eosin (H&E) and MUC5AC, the indicator for the PanIN-1B, which is the preliminary stage of pancreatic cancer, and Ki-67 as a marker of malignant potential, which is thought to be the marker for PanIN-3 (Figure 3C). The results showed that genes including $KRAS^{G12D}$ plasmid-transferred rat groups ($KRAS^{G12D}$, $KRAS^{G12D}$ + *MYC*, $KRAS^{G12D}$ + *MYC* + *YAP*, $KRAS^{G12D}$ + *YAP*) showed a predominantly papillary or micropapillary structure and variable degrees of cytologic and architectural atypia compared to the flat epithelium composed of tall columnar mucin-producing cells in the main pancreatic ducts of rats in groups transferring plasmids, including $KRAS^{WT}$ genes ($KRAS^{WT}$, $KRAS^{WT}$ + *MYC*, $KRAS^{WT}$ + *MYC* + *YAP*) (Figure 3C). Immunohistochemical analyses revealed a significantly higher level of MUC5AC and Ki-67 positively stained cells in groups transferred with $KRAS^{G12D}$-expressing plasmids compared to those of the control groups (WT, NS), YAP-transferred group, and plasmid-transferred groups, including $KRAS^{WT}$ genes ($KRAS^{WT}$, $KRAS^{WT}$ + *MYC*, $KRAS^{WT}$ + *MYC* + *YAP*) (Figures 3C and 3D). These results showed that pancreas-targeted HGD of $KRAS^{G12D}$ gene achieved a microscopic neoplastic lesion of the pancreas with variable mucin production, which is a feature of PanIN, the precursor lesion of invasive PDAC. In addition, while single transfer of the *YAP* gene showed no PanIN development, combinatory transfer with the $KRAS^{G12D}$ gene and *YAP* gene showed statistically higher MUC5AC expression than that of $KRAS^{G12D}$ and $KRAS^{G12D}$ + *MYC*, which indicated that $KRAS^{G12D}$ + *YAP* HGD to the pancreas causes more malignant tumors in wild-type rats (Figures 3C and 3D).

The effect of repeat injection of $KRAS^{G12D}$ on the PanIN progression

Based on the results showing that $KRAS^{G12D}$ increases the atypia of PanIN, oncogenic dosage gain affects the progression of PDAC,[16] and hydrodynamic injection reactivates silenced transgene expression,[32] we examined the effect of repeat HGD of $KRAS^{G12D}$ on malignant transformation and carcinogenesis in the pancreas. *KRAS* expression peaked within a week after pancreas-targeted HGD, and its signal transduction to Akt and Erk was sustained for 4 weeks. The second administration of $KRAS^{G12D}$ was performed 4 weeks after the first administration, and pancreatic tissues were harvested a week after second administration. The pancreatic tissue that received repeat injections of $KRAS^{G12D}$ ($KRAS^{G12D}$/$KRAS^{G12D}$) showed high-grade dysplastic changes in the intraepithelial lesion and atypia (Figure 3E), as evidenced by the immunohistochemical staining of Ki-67 showing a larger number of positively stained cells, while no further increase of MUC5AC stainability was observed (Figure 3F). These results suggest that *KRAS* oncogenic dosage

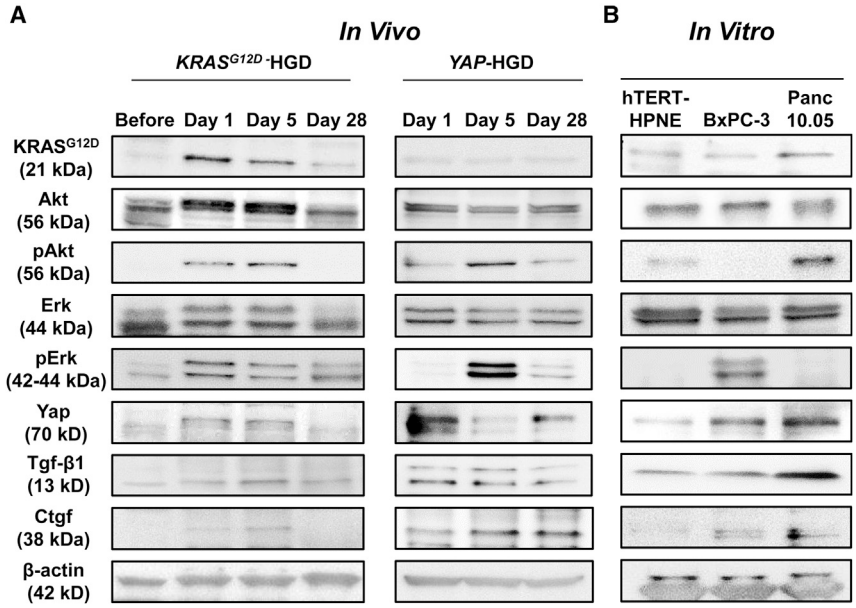

Figure 2. Expression of carcinogenic signaling pathway proteins

(A) Expressions of KRAS^{G12D}, Akt, pAKT, Erk, pErk, Yap, Tgf-β1, Ctgf, and β-actin in the pancreas of *KRAS*^{G12D}-HGD and *YAP*-HGD rats. (B) Expression of the proteins in the cell lines of hTERT-HPNE and hTERT-immortalized pancreatic duct-derived epithelial cell, and BxPC-3 and Panc-10.05, derived from pancreatic adenocarcinoma. HGD, hydrodynamic gene delivery.

gain increased the malignant potential of PanIN and induced atypical lesions (Figure 3C).

The effect of combination and repeat injection of the oncogene to the ADM and PDAC development

As ADM of the pancreas is the origin of PDAC and related to *KRAS*^{G12D} tumorigenesis in pancreas,[15] the effect of repeat injections of the oncogenes is examined on ADM formation. The rat groups of WT, NS/NS, *KRAS*^{G12D}, *KRAS*^{G12D} + *YAP*, *KRAS*^{G12D}/NS, *KRAS*^{G12D}/*KRAS*^{G12D}, *KRAS*^{G12D}/*YAP*, and *KRAS*^{G12D} + *YAP*/*KRAS*^{G12D} + *YAP* (Figure 4A) were histologically examined for ADM development (Figures 4B and 4C). H&E staining showed ADM formation after single *KRAS*^{G12D} administration; its dysplastic change was observed when combined with *YAP* (*KRAS*^{G12D} + *YAP* group), and MUC5AC and Ki-67 positively stained cells showed its increase. This tendency was enhanced by a second injection of genes, and *KRAS*^{G12D}/*KRAS*^{G12D}, *KRAS*^{G12D}/*YAP*, and *KRAS*^{G12D} + *YAP*/*KRAS*^{G12D} + *YAP* showed clear increases in Ki-67 stainability and MUC5AC-positive cells (Figure 4C). Among these groups, *KRAS*^{G12D} + *YAP*/*KRAS*^{G12D} + *YAP* showed severe dysplasia and macroscopic tumors (Figure 4D). We summarized the frequency of macroscopic tumor development in these repeat injection groups in Figure 4E. H&E images of the representative pancreatic tumor including ADM and PDAC lesions in the rat injected with *KRAS*^{G12D} + *YAP*/*KRAS*^{G12D} + *YAP* genes are shown in Figure 4F. ADM lesions are seen in acinar cells and PDAC lesions showing severe dysplasia in ADM lesions with fibrotic changes. While single *KRAS*^{G12D} administration showed ADM in 33% of rats, repeat *KRAS*^{G12D} injection (*KRAS*^{G12D}/*KRAS*^{G12D}) showed significantly increased ADM formation to 66% and PDAC in 33% of rats, thus indicating that ADM formation is related to the dosage of KRAS proteins and activation of the signaling pathway (Figure 4E). *KRAS*^{G12D}/*YAP* showed tumorous lesions macroscopically (Figure 4D); among rats, all showed ADM, 40% showed PDAC, and 20% showed metastatic tumors in lymph nodes and the liver. This indicates that induction of ADM by *KRAS*^{G12D} followed by *YAP* gene transfer activates malignant transformation, which was confirmed by *KRAS*^{G12D} + *YAP*/*KRAS*^{G12D} + *YAP* showing several macroscopically defined tumors in the pancreas (Figure 4D) that were histologically 100% ADM and 80% PDAC. In addition, 30% of rats showed metastatic lesions in the lymph node and liver, subcutaneous lesions, and nervous invasion. Immunohistochemical staining of Ki-67 on the pancreatic tissues of *KRAS*^{G12D} + *YAP*/*KRAS*^{G12D} + *YAP* showed the highest number of positively stained cells among the groups (Figure 4C). In addition, PDAC tumors showed activation of Akt, Erk, Yap, Tgf-β1, and Ctgf, which was consistent with *in vivo* and *in vitro* gene assessment (Figure 4G). Serum levels of CA19-9 were statistically higher in *KRAS*^{G12D}-transferred group and further in *KRAS*^{G12D} and *YAP*-transferred rats (Figure 4H). These results suggest that pancreas-targeted HGD of *KRAS*^{G12D} and *YAP* genes develop pancreatic cancer in wild-type rats in an efficient and timely manner.

Assessment of metastatic tumors

To confirm the histological diagnosis of the metastatic tumors found in rats transferred with *KRAS*^{G12D} and *YAP*, tumors in the liver and lymph node, and subcutaneous lesions and nervous invasion that were diagnosed in the *KRAS*^{G12D} + *YAP*/*KRAS*^{G12D} + *YAP* group rats were assessed on the basis of histological characters determined by H&E, CK7, CK20, Ki-67, and E− and N-cadherin expressions that were related to cancer metastasis[33] (Figure 5). For liver metastasis, the tumor cells surrounded by normal liver cells were stained with an anti-hepatocyte-specific antigen, anti-Hep-Par1. H&E staining showed tubular, small-sized duct-like irregular gland structures with marked nuclear atypia close to the bile duct in the liver. These cells were positively stained for CK7 and CK20 by a marked number of Ki-67-positive cells. Both E- and N-cadherin stained positive (Figure 5A). Subcutaneous metastatic tumors showed a solid white-yellowish mass with small to middle-sized irregular duct-like structures significantly stained positive with Ki-67, CK7, CK20, and N-cadherin (Figure 5B). Lymph node metastasis showed tubular, middle-sized duct-like structures with papillary formations surrounded by lymphoid tissue. The tumor showed marked nuclear atypia stained significantly positive for Ki-67, and the cells were stained

A

Groups	WT	NS	YAP	$KRAS^{WT}$	$KRAS^{WT}$+ MYC	$KRAS^{WT}$+ MYC+YAP	$KRAS^{G12D}$	$KRAS^{G12D}$+ MYC	$KRAS^{G12D}$+ MYC+YAP	$KRAS^{G12D}$+ YAP
NS	–	+	+	+	+	+	+	+	+	+
$KRAS^{WT}$	–	–	–	+	+	+	–	–	–	–
$KRAS^{G12D}$	–	–	–	–	–	–	+	+	+	+
MYC	–	–	–	–	+	+	–	+	+	+
YAP	–	–	+	–	–	+	–	–	+	+

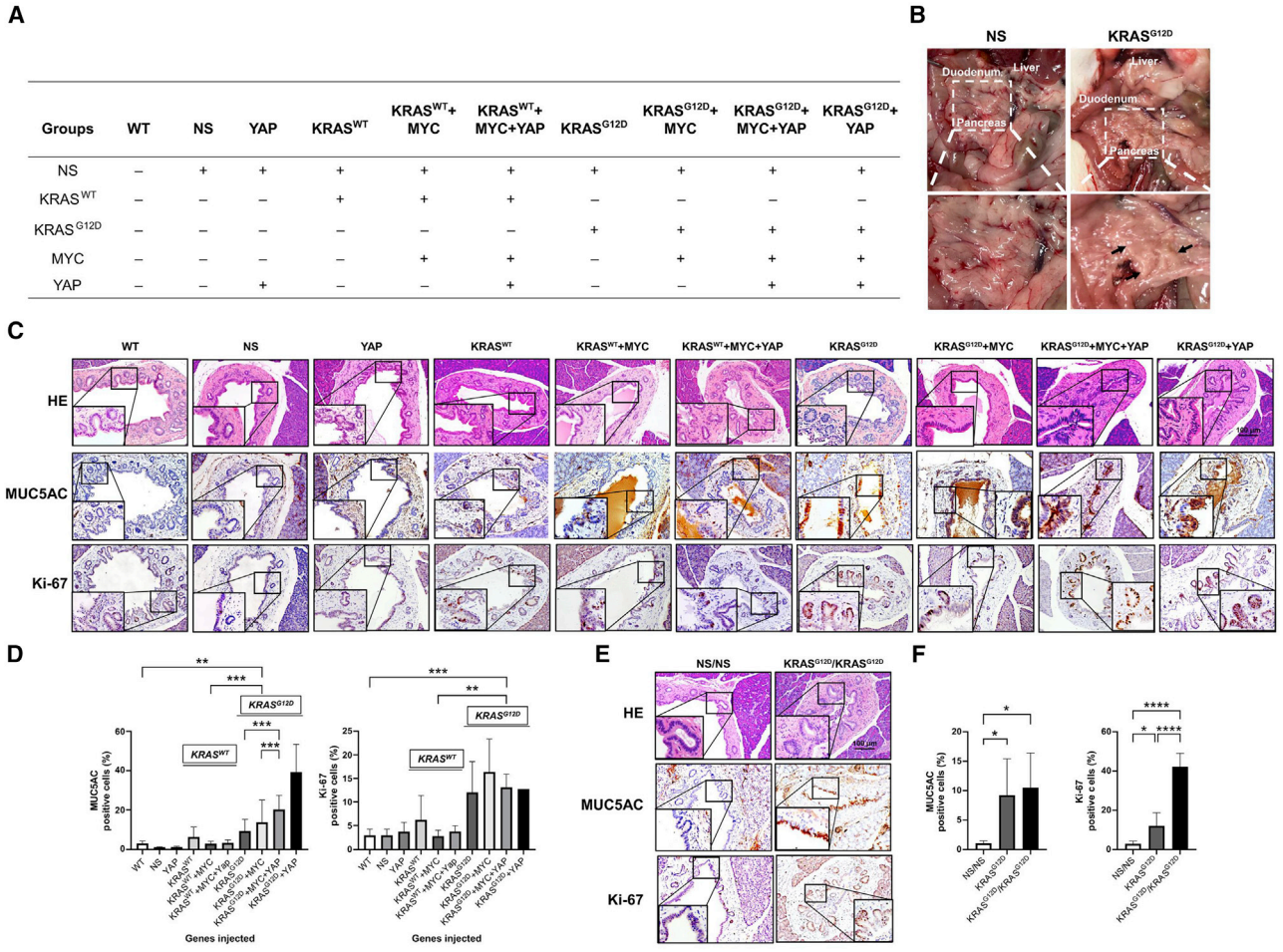

Figure 3. Effect of pancreas-targeted HGD of oncogene on pancreatic tumor development

(A) The list of animal group and genes injected (n = 6 for each group). WT, wild-type; NS, normal saline. (B) Macroscopic nodular lesions in the pancreas of the rats injected with $KRAS^{G12D}$. Black arrows represent nodular lesions. (C) Pancreatic tissues from rats were harvested 4 weeks after the HGD and main pancreatic ducts were stained with HE, MUC5AC, and Ki-67. Representative images of staining are shown for each group. Scale bar represents 100 μm. (D) Five different sections from each of the six rats in all groups (n = 30) were quantitatively analyzed for positively stained cells for MUC5AC and Ki-67 using ImageJ software. The values represent mean ± SEM, $^{**}p < 0.01$, and $^{***}p < 0.001$, and one-way ANOVA with post hoc Tukey's test. (E) Effect of the repeat injection of $KRAS^{G12D}$ on atypical changes in PanIN. Representative images of HE, MUC5AC, and Ki-67 stainings are shown for each group. Scale bar represents 100 μm. (F) Quantitative analyses of MUC5AC and Ki67 positively stained cells in rats with repeat injection conducted analyzed using ImageJ software. The values represent mean ± SEM, $^{*}p < 0.05$, and $^{****}p < 0.0001$, one-way ANOVA with post hoc Tukey's test.

positive for CK7, 20, and N-cadherin (Figure 5C). Direct invasive growth toward the nervous plexus surrounding the pancreas showed papillary formation with severe atypical nuclear formation, which stained positive for CK7, CK20, and both E- and N-cadherin. Tumor cells closely attached to and surrounded by nervous tissues stained positive with S-100 (Figure 5D). These results suggested that PDAC developed from repeat HGD of $KRAS^{G12D}$ + *YAP* transfer achieved metastatic tumor development in the pancreas following malignant transformation by N-cadherin upregulation due to the gene combination. Subcutaneous and lymph node metastases showed a weakly stained E-cadherin, which might be related to the epithelial-mesenchymal transition effect (Figures 5B and 5C).

Effect of YAP on $KRAS^{G12D}$-transferred pancreas

To determine the effect of *YAP* on malignant transformation in the $KRAS^{G12D}$-transferred pancreas, signal transduction was examined *in vitro*. Panc 10.05 was transfected with either a mock or *YAP*-expressing plasmid. *YAP* expression induced TGF-β1 and N-cadherin expressions and decreased E-cadherin expression (Figure 6A). The rats that received single $KRAS^{G12D}$ gene delivery followed by the second NS injection ($KRAS^{G12D}$/NS) showed a higher increase of E-cadherin than that of the control (NS/NS) or $KRAS^{G12D}/KRAS^{G12D}$, $KRAS^{G12D}/YAP$, or $KRAS^{G12D}$ + *YAP*/$KRAS^{G12D}$ + *YAP* groups. However, the N-cadherin showed an increase in $KRAS^{G12D}/YAP$ and $KRAS^{G12D}$ + *YAP*/$KRAS^{G12D}$ + *YAP* rat groups. These results suggest

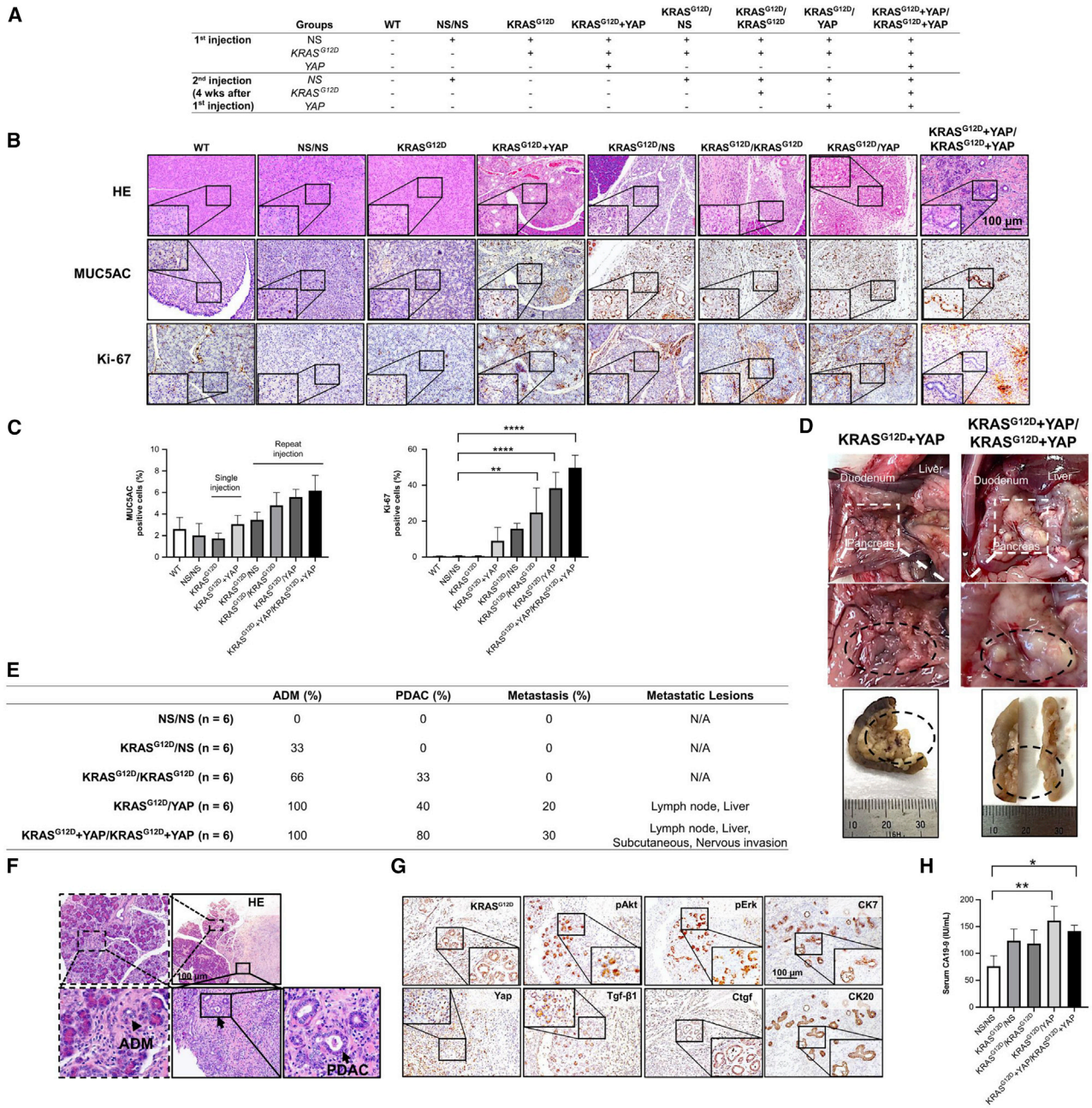

Figure 4. Effect of combination and repeat injection of the oncogene to the ADM and PDAC development

(A) The list of animal group and genes injected (n = 6 for each group). NS, normal saline. (B) Pancreatic tissues from the rat group of WT, *KRAS*^{G12D}, and *KRAS*^{G12D} + *YAP* were harvested 4 weeks after the HGD and NS/NS, *KRAS*^{G12D}/NS, *KRAS*^{G12D}/*KRAS*^{G12D}, *KRAS*^{G12D}/*YAP*, *KRAS*^{G12D} + *YAP*/*KRAS*^{G12D} + *YAP* were harvested a week after the second injections (5 weeks after the first injection). Representative images of HE, MUC5AC, and Ki-67 stainings of ADM lesions of each rat group. Scale bar represents 100 μm. (C) Five different sections from each of the six rats in all groups (n = 30) were quantitatively analyzed for positively stained cells for MUC5AC and Ki-67 using ImageJ software. The values represent mean ± SEM, $^{**}p < 0.01$, and $^{****}p < 0.0001$, one-way ANOVA with post hoc Tukey's test. (D) Macroscopic nodular lesions in the pancreas of the rats injected with *KRAS*^{G12D}/*YAP* and *KRAS*^{G12D} + *YAP*/*KRAS*^{G12D} + *YAP*. Black dotted circles and arrows represent the tumor lesions. (E) The summary of the tumorous lesions found in the repeatedly injected rats. N/A, not applicable. (F) Representative HE stainings of ADM and PDAC tumor lesions in the rat injected with *KRAS*^{G12D} + *YAP*/*KRAS*^{G12D} + *YAP* genes. (G) Representative immunohistochemical staining of Akt, Erk, Yap, TGF-β1, and CTGF in PDAC tumor in *KRAS*^{G12D} + *YAP*/*KRAS*^{G12D} + *YAP* genes injected rats. (H) Serum level of CA19-9 in rat groups (n = 6 from each group). The values represent mean ± SEM, $^{*}p < 0.05$, and $^{****}p < 0.0001$, one-way ANOVA with post hoc Tukey's test.

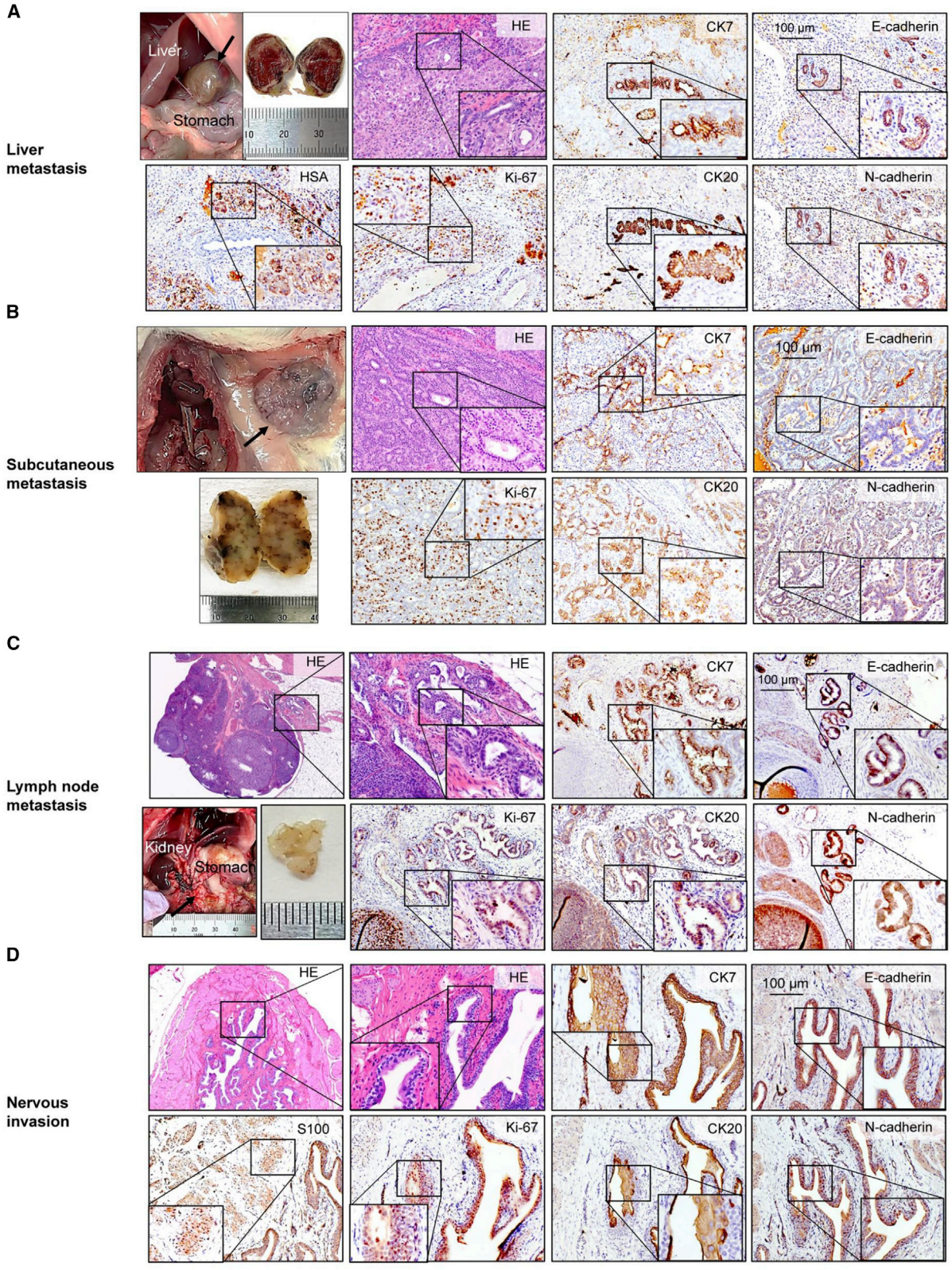

(legend on next page)

that *KRAS*^{G12D} gene transfer induces E-cadherin expression, and additional *YAP* expression could cause a cadherin switch to N-cadherin and promote epithelial-mesenchymal transition leading to increased malignant potential and frequency of metastatic lesions (Figures 6B and 6C). No significant increase or difference in serum aspartate transaminase (AST), alkaline phosphatase (ALP), amylase (AMY), or lactate dehydrogenase (LDH) was observed upon euthanasia (Figure 7).

DISCUSSION

The pancreas consists of acinar, ductal, and pancreatic islet cells, and the ADM is considered to be a major precancerous lesion of PDAC.[15,20-22,34-36] *KRAS*^{G12D} activates *YAP* and *TAZ*,[17,18] which induces continuous ADM followed by PDAC development.[19,28,37] Considering that overexpression of oncogenic genes in the pancreas is necessary to establish PDAC animal models, the complex vascular structures surrounding the pancreas were major concerns for pancreatic gene delivery methods in the past, compared to systemic HGD. Such a technical barrier can be overcome by pancreas-targeted HGD with gene injection into the superior mesenteric vein, a major vein linking to pancreatic veins that lead venous blood to the portal vein.[14] This pancreas-targeted HGD procedure was previously shown by our group to be pancreas specific, safe, and efficient.[14]

In this study, utilizing this procedure, we demonstrated that oncogene delivery to the pancreas led to the development of PDAC models in wild-type rats. The combination and the dosage of the oncogene were related to tumor development. Specifically, a high dosage of *KRAS*^{G12D} in the ductal structures showed PanIN transformation and highly atypical intraepithelial cells, which was supported by previous evidence.[29] The acinar structure showed ADM via *KRAS*^{G12D} transfer, and when combined with *YAP* activation, further malignant transformation to PDAC was marked within 5 weeks of initiation of genes in wild-type rats. This was evidenced by the fact that acinar cells in the pancreas show transformation into ductular cells (ADM) with *KRAS* mutant activation.[15,29] In addition, the combination of *KRAS*^{G12D} and *YAP* genes and the increased dosage by repeat injection in the *KRAS*^{G12D} + *YAP*/*KRAS*^{G12D} + *YAP* group showed transformation from ADM to a significantly malignant PDAC sequence with a high rate of metastatic lesions. Our protein expression assay evidenced activation of *YAP* expression following *KRAS*^{G12D} transfer. These results were supported by evidence showing that *YAP* contributes to the occurrence of ADM and PDAC[17,28] and contributes to the cancer metastasis.[25,31]

In addition, YAP induced EMT[25,26] via the cadherin switch, which refers to expression changes from E-cadherin to N-cadherin that occur during malignant transformation of cancer cells.[27] Our results supported that an *in vivo* switch in *KRAS*^{G12D}- and *YAP*-transferred rats induced metastatic tumors. The fact that the *YAP* single transfer showed no significant tumor development or metastatic changes suggests that the malignant induction of *KRAS*^{G12D} and activation of the pathway through *YAP* addition is important in tumor development. These results supported that pancreatic HGD of the oncogene with appropriate dosage achieved pancreatic cancer model development in the wild-type animal. Further studies are needed to apply this method to other cancer types and animal models. For this purpose, the strategy we reported in various animal species and tissues[38-42] could be considered. The limitations of our study involve the mechanisms of transformation of the gene delivery in normal acinar and pancreatic ductular cells; further studies should include single-cell assays to determine cell type-based phenotypic changes. Such studies will identify effective gene combinations for model development and strengthen the usefulness of this animal model for novel therapy development and biomarker establishment. Additionally, modified procedures might be applied to develop a mouse pancreatic cancer model to improve cost effectiveness.

In summary, pancreas-targeted oncogene HGD induced pancreatic cancer models within 5 weeks in wild-type rats. The tumor occurrence efficacy of this approach depended on the combination and dosage of genes. With molecular signaling activation, the malignant tumor potential increased and exhibited metastatic lesions partly through the cadherin switch. This animal model will speed up pancreatic cancer research for the establishment of the novel treatment strategies and markers for early diagnosis.

MATERIALS AND METHODS

Animals

Animal experiments were approved by and conducted in full compliance with the regulations of the Institutional Animal Care and Use Committee at Niigata University, Niigata, Japan (SA00423). Wistar rats (n = 100, female, 200–250 g) were purchased from Japan SLC (Hamamatsu, Shizuoka, Japan). Rats were housed under the standard conditions of a 12-h light/dark cycle, temperature of 20°C–23°C, and humidity of 45%–55% in pathogen-free facilities. Three rats were housed in a cage and provided with *ad libitum* access to food and water. Rats were given pancreas-targeted hydrodynamic injections as previously described.[14] Under anesthesia using a combination anesthetic prepared with 0.3 mg/kg medetomidine, 2.0 mg/kg midazolam, and 2.5 mg/kg butorphanol, the portal vein in the hilus and superior mesenteric vein were dissected out and isolated. The catheter (SURFLO 22G, Terumo, Shibuya-ku, Tokyo, Japan) was inserted into the superior mesenteric vein with temporary occluding of the blood flow at the portal vein by vessel loops, and the plasmid DNA solution in a volume of 2% body weight (5 μg/mL in saline, 20-μg plasmid in 4 mL for a 200-g rat) was hydrodynamically injected at a flow rate of 1 mL/s (Figure 1). For the HGD of a combination of plasmids, equal amounts of individual plasmids were prepared in a volume of 2% body weight. Therefore, in a 200-g rat simultaneously

Figure 5. Metastatic and invasive lesions developed in the rat pancreatic cancer model

Representative macroscopic and microscopic images of metastatic tumors found in *KRAS*^{G12D} + *YAP*/*KRAS*^{G12D} + *YAP* gene-delivered rats. HE, Ki-67, CK7, CK20, E-cadherin, N-cadherin, HSA, and S100 staining. (A) Liver metastasis. (B) Subcutaneous metastasis. (C) Lymph node metastasis. (D) Direct invasion of the pancreatic tumor to the nervous plexus. HE, hematoxylin and eosin, CK7, Cytokeratin 7, CK20, Cytokeratin 20, HSA, hepatocyte specific antigen. Scale bar represents 100 μm.

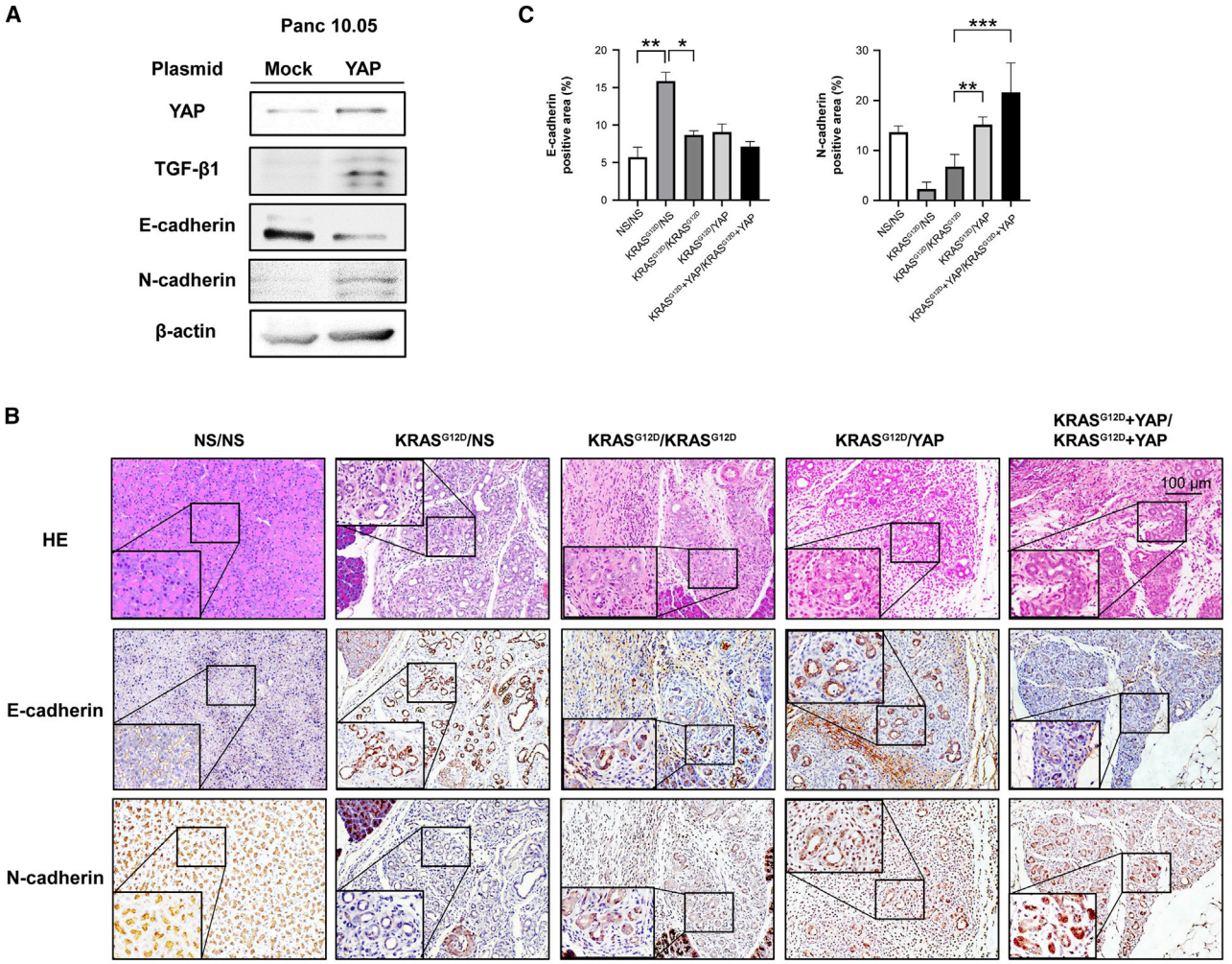

Figure 6. Effect of *YAP* on Cadherin protein expression

(A) Expressions of YAP, TGF-β1, E-cadherin, N-cadherin, and β-actin in mock or YAP-expressing plasmid transfected Panc-10.05 cells. (B) Representative histological images of E- and N-cadherin staining in rat groups. (C) Five different sections from each of the six rats in all groups (n = 30) were quantitatively analyzed for positively stained cells for E- and N-cadherin using ImageJ software. The values represent mean ± SEM, *p < 0.05, **p < 0.01, and ***p < 0.001, one-way ANOVA with post hoc Tukey's test.

receiving two plasmids, 20 μg of each plasmid was diluted in 4 mL of saline solution.

Cells

Human pancreatic adenocarcinoma BxPC-3 (CRL-1687) and Panc 10.05 (CRL-2547) cell lines and human pancreatic duct epithelial cell line hTERT-HPNE (CRL-4023) were purchased from American Type Culture Collection (ATCC, Manassas, VA, USA) and cultured in minimum essential medium containing 10% fetal bovine serum, 100 IU/mL of penicillin, and 100 μg/mL of streptomycin. Cells were incubated in a 5% CO_2 humidified incubator at 37°C.

Plasmids

The YAP-expressing plasmid was constructed using full-length cDNA of human YAP ligated into XbaI restriction sites of the expression vector of the pLIVE vector (Mirus Bio, Madison, WI, USA). The $Kras^{WT}$-expressing plasmid (pCMV6-Entry-KRAS, MR201779), Myc-expressing plasmid (pCMV6-Entry-KRAS G12D, MR201779), and $Kras^{G12D}$-expressing plasmid (pCMV6-Entry-$KRAS^{G12D}$, RC400104) were purchased from OriGene (OriGene Technologies, Rockville, MD, USA). Either a mock or YAP-expressing plasmid were transfected into the Panc 10.05 cell using FuGENE HD Transfection Reagent (Promega, Madison, WI, USA) following the manufacturer's instructions and were harvested 48 h after transfection.

Western blotting

For western blotting analysis, culture cells and a tissue lysate were suspended in phosphate-buffered saline and mixed with equal volumes of lysis buffer, 0.125 M tris-HCl (pH 6.8), 10% sucrose, 10% sodium dodecyl sulfate (SDS), 10% 2-mercaptoethanol, and 0.004%

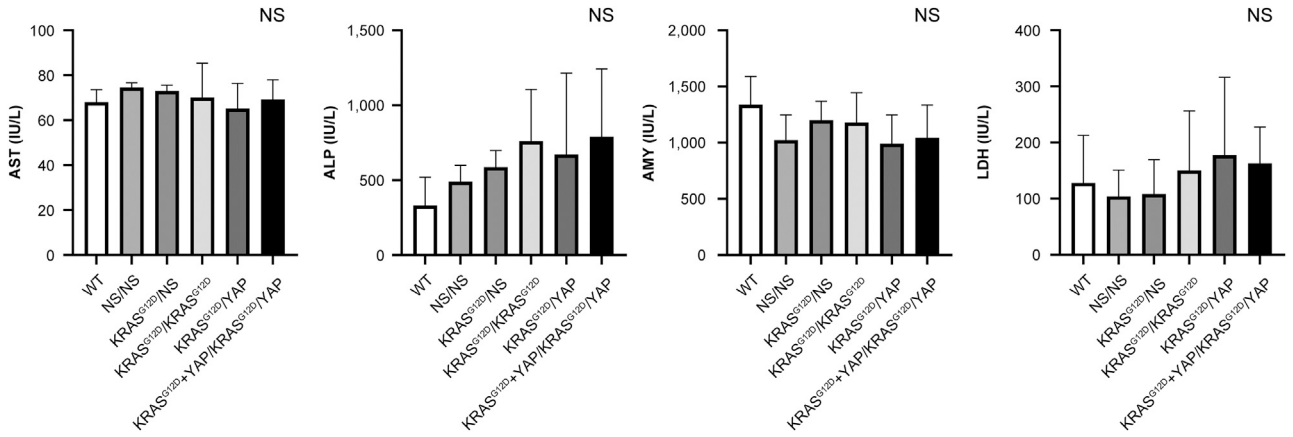

Figure 7. Serum biochemical analyses

Serum biochemical levels of aspartate transaminase (AST), alkaline phosphatase (ALP), amylase (AMY), and lactate dehydrogenase (LDH) upon the euthanasia. The values represent mean ± SEM, *p < 0.05, **p < 0.01, and ***p < 0.001, one-way ANOVA with post hoc Tukey's test.

bromophenol blue. The extract was subjected to 12% SDS-polyacrylamide gel electrophoresis and blotted onto Hybond membranes (GE Healthcare Life Sciences, Pittsburgh, PA, USA). The membranes were blocked by EzBlockChemi (AE-1475; ATTO Corporation Taito-ku, Tokyo, Japan) for 1 h at room temperature and probed with primary antibodies overnight at 4°C. The antibodies used were mouse anti-CTGF antibody (sc-365970, Santa Cruz Biotechnology, Dallas, TX, USA) at 1:100 dilution; mouse anti-β-actin antibody (ab8227, Abcam, Cambridge, UK) at 1:2000 dilution; mouse anti-E-cadherin antibody (ab76055, Abcam) at 1:1,000 dilution; rabbit anti-Ras (mutated G12D) antibody (ab221163, Abcam) at 1:1,000 dilution; rabbit anti-Akt antibody (ab179463, Abcam) at 1:250 dilution; rabbit anti-pAkt antibody (ab192623, Abcam) at 1:500 dilution; rabbit anti-Erk antibody (No. 4695, Cell Signaling Technology, Danvers, MA, USA) at 1:250 dilution; rabbit anti-pErk antibody (No. 4370, Cell Signaling Technology) at 1:500 dilution; rabbit anti-YAP antibody (No. 4912, Cell Signaling Technology) at 1:100 dilution; rabbit anti-TGF-β1 antibody (ab92486, Abcam) at 1:500 dilution; and rabbit anti-N-cadherin antibody (ab18203, Abcam) at 1:1,000 dilution. Then, the membrane was incubated with secondary antibodies of anti-mouse (NA931-1ML; GE Healthcare Life Sciences) or anti-rabbit (NA934-1ML; GE Healthcare Life Sciences) antibody conjugated with horseradish peroxidase. Protein bands were visualized using the ECL plus Western Blotting Detection System (GE Healthcare Life Sciences).

Histological analysis

Tissue samples for immunohistochemical staining were collected at the appropriate time points after the procedures and then fixed in 10% formalin upon tissue collection before embedding in paraffin. Five sections from the pancreas or tumors (10 μm) were collected from each of the 10 rats in the group, and standard H&E staining and immunohistochemistry were performed. For immunohistochemical staining, anti-MUC5AC antibody (ab3649, Abcam) at 1:200 dilution; anti-CTGF antibody (sc-365970, Santa Cruz Biotechnology) at 1:1,000 dilution; anti-CK7 antibody (ab9021, Abcam) at 1:250 dilution; anti-E-cadherin antibody (ab76055, Abcam) at 1:1,000 dilution; and anti-hepatocyte specific antigen antibody (sc-58693, Santa Cruz Biotechnology) at 1:50 dilution with Vectastain Elite ABC mouse IgG kit (PK-6102, Vector Laboratories, Burlingame, CA, USA) and DAB chromogen tablets (Muto Pure Chemicals, Tokyo, Japan); anti-Ki67 antibody (ab15580, Abcam) at 1:1,000 dilution; anti-Ras (mutated G12D) antibody (ab221163, Abcam) at 1:250 dilution; anti-pAkt antibody (ab179463, Abcam) at 1:100 dilution; anti-TGF-β1 antibody (ab92486, Abcam) at 1:100 dilution; anti-pErk antibody (No. 4370, Cell Signaling Technology) at 1:250 dilution; anti-YAP antibody (No. 4912, Cell Signaling Technology) at 1:250 dilution; anti-CK20 antibody (ab76126, Abcam) at 1:100 dilution; anti-N-cadherin antibody (ab18203, Abcam) at 1:1,000 dilution; and anti-S100 antibody (ab34686, Abcam) at 1:500 dilution with Vectastain Elite ABC rabbit IgG kit (PK-6101, Vector Laboratories) and DAB chromogen tablets (Muto Pure Chemicals, Tokyo, Japan) were employed. Then, images of each tissue section were captured randomly, and quantitative analysis was performed with ImageJ software (version 1.6.0_20; National Institutes of Health, Bethesda, MD, USA) with RGB-based protocol, as reported previously.[43]

Biochemical analysis

Blood samples were collected from each rat before euthanasia, and serum biochemical analyses of AST, ALP, AMY, and LDH were performed (Oriental Yeast, Shiga, Japan). The serum level of carbohydrate antigen 19-9 (CA19-9) was analyzed by enzyme-linked immunosorbent assay using Rat Sialylated Lewis a/CA 19-9 ELISA Kit (LS-F27918, LSBio, Seattle, WA, USA).

Statistical analyses

Histological and serum biochemical factors were statistically evaluated by one-way analysis of variance (ANOVA) followed by Bonferroni's multiple comparison test using GraphPad Prism7 software

(version 7.04; MDF, Tokyo, Japan). $p \leq 0.05$ denoted statistical significance.

Data availability statement

The authors confirm that the data supporting the findings of this study are available within the article.

ACKNOWLEDGMENTS

The authors would like to thank Takao Tsuchida in the Division of Gastroenterology and Hepatology at Niigata University for his excellent assistance in the histological analyses. The authors would also like to thank Nobuyoshi Fujisawa, Kanako Oda, Shuko Adachi, Toshikuni Sasaoka, and all staff members at the Division of Laboratory Animal Resources in Niigata University. The research in the authors' laboratory was supported in part by a Grant-in-Aid for Scientific Research from the Japanese Society for the Promotion of Sciences 22890064, 23790595, 26860354, 17K09408, and 20K08379 to Kamimura K; 18K15745 and 21K07889 to Ikarashi S; 20K22800 to Ogawa K; and 21K07910 to Hayashi K; Takara Bio Award from JSGCT to Kamimura K, and a research grant from the Pancreas Research Foundation of Japan to Kamimura K.

AUTHOR CONTRIBUTIONS

O.S., K.K., Y.T., and K.O. contributed to the study conception and design. Material preparation, data collection, and analysis were performed by O.S., K.K., Y.T., K.O., T.O., C.Y., S.M., A.K., H.A., S.I., K.H., T.Y., and S.T. The first draft of the manuscript was written by O.S., K.K., and S.T., and all authors read and approved the final manuscript.

DECLARATION OF INTERESTS

The authors declare that they have no conflict of interest.

REFERENCES

1. Siegel, R.L., Miller, K.D., Fuchs, H.E., and Jemal, A. (2021). Cancer statistics, 2021. CA Cancer J. Clin. *71*, 7–33.
2. Ryan, D.P., Hong, T.S., and Bardeesy, N. (2014). Pancreatic adenocarcinoma. N. Engl. J. Med. *371*, 1039–1049.
3. Longnecker, D.S., Memoli, V., and Pettengill, O.S. (1992). Recent results in animal models of pancreatic carcinoma: histogenesis of tumors. Yale J. Biol. Med. *65*, 457–464, discussion 465–9.
4. Rao, M.S. (1987). Animal models of exocrine pancreatic carcinogenesis. Cancer Metastasis Rev. *6*, 665–676.
5. Hayashi, Y., and Hasegawa, T. (1971). Experimental pancreatic tumor in rats after intravenous injection of 4-hydroxyaminoquinoline 1-oxide. Gan *62*, 329–330.
6. Reddy, J.K., and Rao, M.S. (1977). Malignant tumors in rats fed nafenopin, a hepatic peroxisome proliferator. J. Natl. Cancer Inst. *59*, 1645–1650.
7. Reddy, J.K., and Qureshi, S.A. (1979). Tumorigenicity of the hypolipidaemic peroxisome proliferator ethyl-alpha-p-chlorophenoxyisobutyrate (clofibrate) in rats. Br. J. Cancer *40*, 476–482.
8. Longnecker, D.S., Curphey, T.J., Lilja, H.S., French, J.I., and Daniel, D.S. (1980). Carcinogenicity in rats of the nitrosourea amino acid N delta-(N-methyl-N-nitrosocarbamoyl)-L-ornithine. J. Environ. Pathol. Toxicol. *4*, 117–129.
9. Kong, K., Guo, M., Liu, Y., and Zheng, J. (2020). Progress in animal models of pancreatic ductal adenocarcinoma. J. Cancer *11*, 1555–1567.
10. Tanaka, H., Fukamachi, K., Futakuchi, M., Alexander, D.B., Long, N., Tamamushi, S., Minami, K., Seino, S., Ohara, H., Joh, T., et al. (2010). Mature acinar cells are refractory to carcinoma development by targeted activation of Ras oncogene in adult rats. Cancer Sci. *101*, 341–346.
11. Park, J.S., Kim, B.H., Park, S.G., Jung, S.Y., Lee, D.H., and Son, W.C. (2013). Induction of rat liver tumor using the Sleeping Beauty transposon and electroporation. Biochem. Biophys. Res. Commun. *434*, 589–593.
12. Kamimura, K., Yokoo, T., Abe, H., and Terai, S. (2019). Gene therapy for liver cancers: current status from basic to clinics. Cancers (Basel) *11*, 1865.
13. Kamimura, K., Yokoo, T., Abe, H., Sakai, N., Nagoya, T., Kobayashi, Y., Ohtsuka, M., Miura, H., Sakamaki, A., Kamimura, H., et al. (2020). Effect of diphtheria toxin-based gene therapy for hepatocellular carcinoma. Cancers (Basel) *12*, 472.
14. Ogawa, K., Kamimura, K., Kobayashi, Y., Abe, H., Yokoo, T., Sakai, N., Nagoya, T., Sakamaki, A., Abe, S., Hayashi, K., et al. (2017). Efficacy and safety of pancreas-targeted hydrodynamic gene delivery in rats. Mol. Ther. Nucleic Acids *9*, 80–88.
15. Chuvin, N., Vincent, D.F., Pommier, R.M., Alcaraz, L.B., Gout, J., Caligaris, C., Yacoub, K., Cardot, V., Roger, E., Kaniewski, B., et al. (2017). Acinar-to-ductal metaplasia induced by transforming growth factor beta facilitates $KRAS^{G12D}$-driven pancreatic tumorigenesis. Cell Mol. Gastroenterol. Hepatol. *4*, 263–282.
16. Mueller, S., Engleitner, T., Maresch, R., Zukowska, M., Lange, S., Kaltenbacher, T., Konukiewitz, B., Öllinger, R., Zwiebel, M., Strong, A., et al. (2018). Evolutionary routes and KRAS dosage define pancreatic cancer phenotypes. Nature *554*, 62–68.
17. Gruber, R., Panayiotou, R., Nye, E., Spencer-Dene, B., Stamp, G., and Behrens, A. (2016). YAP1 and TAZ control pancreatic cancer initiation in mice by direct up-regulation of JAK-STAT3 signaling. Gastroenterology *151*, 526–539.
18. Roy, N., and Hebrok, M. (2015). Regulation of cellular identity in cancer. Dev. Cell. *35*, 674–684.
19. Macgregor-Das, A.M., and Iacobuzio-Donahue, C.A. (2013). Molecular pathways in pancreatic carcinogenesis. J. Surg. Oncol. *107*, 8–14.
20. Pan, F.C., Bankaitis, E.D., Boyer, D., Xu, X., Van de Casteele, M., Magnuson, M.A., Heimberg, H., and Wright, C.V. (2013). Spatiotemporal patterns of multipotentiality in Ptf1a-expressing cells during pancreas organogenesis and injury-induced facultative restoration. Development *140*, 751–764.
21. Murtaugh, L.C., and Keefe, M.D. (2015). Regeneration and repair of the exocrine pancreas. Annu. Rev. Physiol. *77*, 229–249.
22. Jensen, J.N., Cameron, E., Garay, M.V., Starkey, T.W., Gianani, R., and Jensen, J. (2005). Recapitulation of elements of embryonic development in adult mouse pancreatic regeneration. Gastroenterology *128*, 728–741.
23. Yang, S., Zhang, L., Purohit, V., Shukla, S.K., Chen, X., Yu, F., Fu, K., Chen, Y., Solheim, J., Singh, P.K., et al. (2015). Active YAP promotes pancreatic cancer cell motility, invasion and tumorigenesis in a mitotic phosphorylation-dependent manner through LPAR3. Oncotarget *6*, 36019–36031.
24. Diep, C.H., Zucker, K.M., Hostetter, G., Watanabe, A., Hu, C., Munoz, R.M., Von Hoff, D.D., and Han, H. (2012). Down-regulation of Yes Associated Protein 1 expression reduces cell proliferation and clonogenicity of pancreatic cancer cells. PLoS One *7*, e32783.
25. Warren, J.S.A., Xiao, Y., and Lamar, J.M. (2018). YAP/TAZ Activation as a target for treating metastatic cancer. Cancers (Basel) *10*, 115.
26. Datta, A., Deng, S., Gopal, V., Yap, K.C., Halim, C.E., Lye, M.L., Ong, M.S., Tan, T.Z., Sethi, G., Hooi, S.C., et al. (2021). Cytoskeletal dynamics in epithelial-mesenchymal transition: insights into therapeutic targets for cancer metastasis. Cancers (Basel) *13*, 1882.
27. Park, J., Kim, D.H., Shah, S.R., Kim, H.N., Kshitiz, Kim, P., Quiñones-Hinojosa, A., and Levchenko, A. (2019). Switch-like enhancement of epithelial-mesenchymal transition by YAP through feedback regulation of WT1 and Rho-family GTPases. Nat. Commun. *10*, 2797.
28. Zhang, W., Nandakumar, N., Shi, Y., Manzano, M., Smith, A., Graham, G., Gupta, S., Vietsch, E.E., Laughlin, S.Z., Wadhwa, M., et al. (2014). Downstream of mutant KRAS, the transcription regulator YAP is essential for neoplastic progression to pancreatic ductal adenocarcinoma. Sci. Signal. *7*, ra42.
29. Storz, P., and Crawford, H.C. (2020). Carcinogenesis of pancreatic ductal adenocarcinoma. Gastroenterology *158*, 2072–2081.

30. Waters, A.M., Khatib, T.O., Papke, B., Goodwin, C.M., Hobbs, G.A., Diehl, J.N., Yang, R., Edwards, A.C., Walsh, K.H., Sulahian, R., et al. (2021). Targeting p130Cas- and microtubule-dependent MYC regulation sensitizes pancreatic cancer to ERK MAPK inhibition. Cell Rep. *35*, 109291.

31. Salcedo Allende, M.T., Zeron-Medina, J., Hernandez, J., Macarulla, T., Balsells, J., Merino, X., Allende, H., Tabernero, J., and Ramon Y Cajal, S. (2017). Overexpression of Yes Associated Protein 1, an independent prognostic marker in patients with pancreatic ductal adenocarcinoma, correlated with liver metastasis and poor prognosis. Pancreas *46*, 913–920.

32. Nishikawa, M., Nakayama, A., Takahashi, Y., Fukuhara, Y., and Takakura, Y. (2008). Reactivation of silenced transgene expression in mouse liver by rapid, large-volume injection of isotonic solution. Hum. Gene Ther. *19*, 1009–1020.

33. Mrozik, K.M., Blaschuk, O.W., Cheong, C.M., Zannettino, A.C.W., and Vandyke, K. (2018). N-cadherin in cancer metastasis, its emerging role in haematological malignancies and potential as a therapeutic target in cancer. BMC Cancer *18*, 939.

34. Tu, Q., Yang, D., Zhang, X., Jia, X., An, S., Yan, L., Dai, H., Ma, Y., Tang, C., Tong, W., et al. (2019). A novel pancreatic cancer model originated from transformation of acinar cells in adult tree shrew, a primate-like animal. Dis. Model. Mech. *12*, dmm038703.

35. Maresch, R., Mueller, S., Veltkamp, C., Öllinger, R., Friedrich, M., Heid, I., Steiger, K., Weber, J., Engleitner, T., Barenboim, M., et al. (2016). Multiplexed pancreatic genome engineering and cancer induction by transfection-based CRISPR/Cas9 delivery in mice. Nat. Commun. *7*, 10770.

36. Kopp, J.L., von Figura, G., Mayes, E., Liu, F.F., Dubois, C.L., Morris, J.P., Pan, F.C., Akiyama, H., Wright, C.V., Jensen, K., et al. (2012). Identification of Sox9-dependent acinar-to-ductal reprogramming as the principal mechanism for initiation of pancreatic ductal adenocarcinoma. Cancer Cell *22*, 737–750.

37. Dimcevski, G., Kotopoulis, S., Bjånes, T., Hoem, D., Schjøtt, J., Gjertsen, B.T., Biermann, M., Molven, A., Sorbye, H., McCormack, E., et al. (2016). A human clinical trial using ultrasound and microbubbles to enhance gemcitabine treatment of inoperable pancreatic cancer. J. Control. Release *243*, 172–181.

38. Kamimura, K., Suda, T., Xu, W., Zhang, G., and Liu, D. (2009). Image-guided, lobe-specific hydrodynamic gene delivery to swine liver. Mol. Ther. *17*, 491–499.

39. Kamimura, K., Zhang, G., and Liu, D. (2010). Image-guided, intravascular hydrodynamic gene delivery to skeletal muscle in pigs. Mol. Ther. *18*, 93–100.

40. Kamimura, K., Suda, T., Zhang, G., Aoyagi, Y., and Liu, D. (2013). Parameters affecting image-guided, hydrodynamic gene delivery to swine liver. Mol. Ther. Nucleic Acids *2*, e128.

41. Kamimura, K., Kanefuji, T., Yokoo, T., Abe, H., Suda, T., Kobayashi, Y., Zhang, G., Aoyagi, Y., and Liu, D. (2014). Safety assessment of liver-targeted hydrodynamic gene delivery in dogs. PLoS One *9*, e107203.

42. Suda, T., Suda, K., and Liu, D. (2008). Computer-assisted hydrodynamic gene delivery. Mol. Ther. *16*, 1098–1104.

43. Vrekoussis, T., Chaniotis, V., Navrozoglou, I., Dousias, V., Pavlakis, K., Stathopoulos, E.N., and Zoras, O. (2009). Image analysis of breast cancer immunohistochemistry-stained sections using ImageJ: an RGB-based model. Anticancer Res. *29*, 4995–4998.